Since January 2020 Elsevier has created a COVID-19 resource centre with free information in English and Mandarin on the novel coronavirus COVID-19. The COVID-19 resource centre is hosted on Elsevier Connect, the company's public news and information website.

Virology 539 (2020) 121–128

Contents lists available at ScienceDirect

Virology

journal homepage: www.elsevier.com/locate/virology

EGR1 upregulation following Venezuelan equine encephalitis virus infection is regulated by ERK and PERK pathways contributing to cell death

Bibha Dahal[a], Shih-Chao Lin[a], Brian D. Carey[a], Jonathan L. Jacobs[b,c], Jonathan D. Dinman[d], Monique L. van Hoek[a], Andre A. Adams[e], Kylene Kehn-Hall[a,*]

[a] National Center for Biodefense and Infectious Diseases, School of Systems Biology, George Mason University, Manassas, VA, USA
[b] QIAGEN Bioinformatics, Aarhus, Denmark
[c] QIAGEN Bioinformatics, Maryland, USA
[d] Department of Cell Biology and Molecular Genetics, University of Maryland, College Park, MD, USA
[e] Naval Research Laboratory, Washington, DC, USA

ARTICLE INFO

Keywords:
EGR1
Early growth response 1
Venezuelan equine encephalitis virus
VEEV
Apoptosis
ERK
PERK
Unfolded protein response
UPR
Alphavirus

ABSTRACT

Venezuelan equine encephalitis virus (VEEV) is a neurotropic virus that causes significant disease in both humans and equines. Here we characterized the impact of VEEV on signaling pathways regulating cell death in human primary astrocytes. VEEV productively infected primary astrocytes and caused an upregulation of early growth response 1 (EGR1) gene expression at 9 and 18 h post infection. EGR1 induction was dependent on extracellular signal-regulated kinase1/2 (ERK1/2) and protein kinase R (PKR)-like endoplasmic reticulum kinase (PERK), but not on p38 mitogen activated protein kinase (MAPK) or phosphoinositide 3-kinase (PI3K) signaling. Knockdown of EGR1 significantly reduced VEEV-induced apoptosis and impacted viral replication. Knockdown of ERK1/2 or PERK significantly reduced EGR1 gene expression, dramatically reduced viral replication, and increased cell survival as well as rescued cells from VEEV-induced apoptosis. These data indicate that EGR1 activation and subsequent cell death are regulated through ERK and PERK pathways in VEEV infected primary astrocytes.

1. Introduction

Venezuelan equine encephalitis virus (VEEV) is an encephalitogenic *Alphavirus* that belongs to the family *Togaviridae*. VEEV causes febrile illness in humans, characterized by fever, malaise, and vomiting. Infection can progress to the central nervous system (CNS), causing neurological symptoms, including confusion, ataxia, and seizures. VEEV infection initiates a biphasic disease: a peripheral phase, where viral replication occurs in the lymphoid and myeloid tissues, and a neurotrophic phase, where viral replication progresses to the CNS resulting in neuropathology and in some cases fatal encephalitis. Encephalitis develops in approximately 4% of cases with an overall mortality of 1–2% (Schäfer et al., 2011).

VEEV is endemic in parts of South, Central and North America causing periodic outbreaks of disease. Over 200,000 humans were infected with an epizootic strain (subtype IAB) of VEEV during the 1960's outbreak in Columbia (Weaveret al, 2004). VEEV is classified as a biosafety level-3 (BSL-3) select agent by both the Centers for Disease Control and Prevention and the United States Department of Agriculture and as a Category B priority pathogen by the National Institute of Allergy and Infectious Diseases due to its ease of aerosolization, low infectious dose, and potential to cause a major public health threat in the United States (Croddy). In addition, VEEV was previously weaponized by the former Soviet Union and the United States. Various laboratory accidents have been recorded and reports from animal studies indicate that aerosolized VEEV is highly infectious and could possibly result in higher mortality than that noted with natural infection (Franz et al., 2001; Hanson et al., 1967). Currently, there are no FDA approved therapeutics available for the treatment and prevention of VEEV in humans; military personnel and at risk lab workers are vaccinated with the TC-83 strain (Paessler and Weaver, 2009), which is an attenuated strain from the virulent VEEV Trinidad donkey (TrD) strain after 83 serial passages in guinea pig heart cells (Kinney et al., 1993). Since the TC-83 strain of VEEV is attenuated it can be utilized at BSL-2 as a model to better understand VEEV replication and to assist in therapeutic discovery.

In vivo studies of murine brain suggest that astrocytes are an important target for establishing VEEV infection in the CNS (Peng et al.,

* Corresponding author.
E-mail address: kkehnhal@gmu.edu (K. Kehn-Hall).

https://doi.org/10.1016/j.virol.2019.10.016
Received 27 May 2019; Received in revised form 2 October 2019; Accepted 28 October 2019
Available online 31 October 2019

2013). Astrocytes are the major glial cells of the CNS, outnumbering neurons by over five-fold. These cells play an important role in many normal CNS functions, including, supporting and protecting neurons, maintaining homeostatic balance by regulating neurotransmitter and ion concentrations, and providing structural support. Several neurotrophic viruses are capable of infecting astrocytes leading to severe neurological complications and CNS damage (Bender et al., 2012). It is now well established that VEEV infection causes inflammation of CNS. Infection of primary astrocytes with VEEV subtype IAB V3000 (molecular clone of VEEV TrD (Grieder et al., 1995)) or attenuated V3010 (cloned avirulent mutant, E2 76Glu to Lys (Aronson et al., 2000)) released pro-inflammatory cytokines, TNF-α, and iNOS. The attenuated TC-83 strain of VEEV induces pro-inflammatory cytokines such as IFN-ɣ, IL-1β, IL-6, IL-8, IL-12, and TNF-α, which contribute to the inflammatory microenvironment (Peng et al., 2013; Schoneboom et al., 2000).

We previously demonstrated that infection of U87MG astrocytoma cells with the VEEV TrD strain, epidemic subtype IAB, induces early growth response 1 (EGR1) mRNA and protein expression leading to cell death via the unfolded protein response (UPR) (Baer et al., 2016). The protein kinase R (PKR)-like endoplasmic reticulum kinase (PERK) arm of the UPR was found to be activated following VEEV infection. EGR1 belongs to the family of immediate early genes, and is a Cys2-His2-type zinc-finger transcription factor associated with growth, cell survival, and apoptosis. Various extracellular stimuli are capable of activating EGR1 mediating cellular stress responses and being a transcription factor, EGR1 promotes the expression of other genes, as well as its own transcription (Pagel and Deindl, 2011). Furthermore, EGR1 is a major mediator and regulator of synaptic plasticity and neuronal activity in both physiological and pathological conditions (Duclot and Kabbaj, 2017a).

EGR1 is upregulated in astrocytes during other viral infections, including murine coronavirus infection of U87MG astrocytoma cells (Schoneboom et al., 2000), HIV Tat expression in U87MG cells, and HIV-infection of mouse primary astrocytes (Fan, 2011). These studies suggest that EGR1 upregulation may be a conserved stress response induced in astrocytes following viral infection. Our prior results demonstrated that the loss of EGR1 resulted in lower susceptibility to VEEV-induced cell death, indicating that EGR1 modulates pro-apoptotic pathways following infection (Baer et al., 2016). However, U87MG cells are a glioma cell line, a characteristic which could potentially lead to significant differences from primary astrocytes in responding to viral infection and replication. Therefore, in the current study, human primary astrocytes were used to determine if EGR1 is activated in primary cells upon VEEV TC-83 infection and to confirm what signaling pathway(s) actively contribute to EGR1 upregulation and apoptosis in VEEV-infected cells.

2. Material and methods

2.1. Cell culture

Primary human astrocytes were obtained from Lonza and maintained in Astrocyte growth medium (AGM) BulletKit (CC-3187 & CC-4123). Vero (ATCC CCL-81) cells were maintained in Dulbecco's modified minimum essential medium (DMEM) supplemented with 10% fetal bovine serum (FBS), 1% L-glutamine, and 1% penicillin/streptomycin. All cells were maintained at 37 °C with 5% CO_2.

2.2. Viruses and infections

VEEV TC-83 was obtained from BEI Resources. For viral infections, cells were plated in a 6-well (4×10^5 cells/well) or a 12-well (2×10^5 cells/well) plate and incubated overnight. Next day, cells were infected at the specified multiplicity of infection (MOI). Cells were infected for 1 h at 37 °C and rocked every 15 min to ensure adequate coverage. The cells were then washed with phosphate-buffered saline (PBS), and complete growth medium was added back to the cells. Viral supernatants and cells were collected at various times post-infection for further analysis. To determine viral titers, astrocytes were seeded in a 96-well plate at 15,000 cells per well and allowed to incubate overnight at 37 °C and 5% CO_2. Treatments and infections were performed as described above. Supernatants were collected at the indicated time points and stored at −80 °C until use. Viral titers were determined by crystal violet plaque assay using Vero cells as previously described (Au - Baer and Au - Kehn-Hall, 2014).

2.3. RNA isolation and quantitative RT-PCR

Total RNA extracted from mock-infected or VEEV TC-83-infected astrocytes [3, 6, 9, and 18 h post infection (hpi)] was isolated using the RNeasy mini kit (Qiagen) according to the manufacturer's instructions. Real-time quantitative PCR (RT-qPCR) was performed using the StepOnePlus™ Real-Time PCR System (Life Technologies). TaqMan Gene Expression Assays were used for EGR1 (Hs00152928_m1) or 18S (Hs99999901_s1). Fold changes were calculated relative to 18S ribosomal RNA and normalized to mock samples using the ΔΔCt method. Detection of viral RNA in astrocytes was determined by RT-qPCR with Invitrogen's RNA UltraSense™ One-Step Quantitative RT-PCR System using Integrated DNA Technologies primer pairs (forward, GTGTGAC CAAATGACTG, and reverse, ACCGTTGACGACTATAC) and TaqMan probe (5′-6-carboxyfluorescein TCGTCCGCACTGACATCTGTTGC-carboxytetramethylrhodamine-3′) against the viral RNA packaging signal (nt 1057 to 1154) as described previously (Kim et al., 2011). The absolute quantification was done using StepOne software v2.3 based on the threshold cycle relative to the standard curve. The standard curve was determined using serial dilutions of VEEV TC-83 RNA at known concentrations.

2.4. Western blot analyses

Protein lysates were collected using Blue Lysis Buffer and analyzed by western blot as previously described (Austin et al., 2012). The recipe for Blue Lysis Buffer consists of: 25 ml 2x Novex Tris-Glycine Sample Loading Buffer SDS (Invitrogen, Cat# LC2676), 20 ml T-PER Tissue Protein Extraction Reagent (ThermoFisher, Cat# 78510), 200 µl 0.5M EDTA pH 8.0, 2–3 complete Protease Cocktail tablets for 50 ml, 80 µl 0.1M Na_3VO_4, 400 µl 0.1M NaF, 1.3 ml 1M dithiothreitol. Briefly, primary antibodies against capsid of Venezuelan equine encephalitis virus, TC-83 (Subtype IA/B) Capsid (antiserum, Goat) (BEI resources, NR-9403), EGR1 (44D5) (Cell Signaling, Cat# 4154S), ERK1/2 (Cell Signaling, Cat# 4695S), PERK (C33E10) (Cell Signaling, Cat# 3192S), or horse radish peroxidase (HRP)-conjugated β-actin antibody (Abcam, Cat# ab49900) were diluted in 3% milk solution per the manufacturer's recommended dilutions followed by the addition of the appropriate secondary antibody either anti-rabbit HRP-conjugated (Cell Signaling, Cat# 7074), or anti-goat HRP-conjugated antibody. PDVF membranes were imaged on a Chemidoc XRS molecular imager (Bio-Rad) using the SuperSignal West Femto Maximum Sensitivity Substrate kit (ThermoFisher, Cat# 34095).

2.5. Inhibitor treatments

Cells were treated prior to viral infection (pre-treated) and following the 1 h viral infection (post-treated) with either dimethyl sulfoxide (DMSO), MEK/ERK inhibitor (PD0325901, MedChem Express, Cat# HY-10254), p38MAPK inhibitor (SB203580, Selleckchem, Cat# S1076), PI3K inhibitor (PI-103), or PERK inhibitor (GSK2606414, EMD Millipore, Cat# 516535). The DMSO concentration was equal to the volume of the inhibitors added to the medium and always less than 0.1% of the final sample volume.

2.6. siRNA transfections

Astrocytes seeded at 2.5 × 10^5 cells per well in a 12-well plate were transfected with 50 nM siGenome SMARTpool EGR1 (Dharmacon, Cat# M-006526-01), 100 nM SignalSilence® p44/42 MAPK (Erk1/2) siRNA (Cell Signaling, Cat# 6560S), 100 nM SignalSilence® PERK siRNA I (Cell Signaling, Cat# 9024S), or AllStar negative-control small interfering RNA (Qiagen, Cat# 1027280), using 1.2 µl of the DharmaFECT 1 transfection reagent (Dharmacon, Cat# T-2001-02). At 48 h post-transfection, cells were infected with VEEV TC-83 (MOI 5) for 1 h. After infection the medium was replaced with fresh medium. At 18hpi or 36hpi lysates were collected for analysis.

2.7. Cell viability assays

For cell viability assays, astrocytes were cultured as described above in 96-well white walled plate (Corning, Cat# 3903) and transfected with siRNAs followed by mock infection or VEEV TC-83 infection at an MOI of 5 for 36hpi. ATP production was measured as an indication of cell viability using the Promega's CellTiter-Glo assay (Cat# G7570).

2.8. Caspase–Glo 3/7 assays

For Caspase-Glo 3/7 assays, astrocytes were cultured as described above in a 96-well white walled plate and transfected with siRNAs for 48 h followed by mock infection or VEEV TC-83 infection at MOI of 5 for 18 or 36hpi. Caspase activity was measured using Promega's Caspase-Glo 3/7 assay (Cat# G8090), following the manufacturer's instructions.

2.9. Statistics

Unless otherwise noted, all statistical analysis was calculated using an unpaired, two-tailed Student's t-test using Graphpad's QuickCalcs software. All graphs contain the mean and standard deviations with an n = 3 unless otherwise mentioned.

3. Results

3.1. Replication of VEEV in human primary astrocytes

Experiments were performed to confirm the ability of VEEV to replicate in monolayer cultures of primary human astrocytes. Cells were infected with VEEV at an MOI of 0.1, 1, and 5. Viral replication and cytopathic effects (CPE) were determined at 3, 6, 9, 18, 24, and 48 h post infection (hpi). VEEV replicated effectively in human primary astrocytes reaching maximum titers at all MOIs by 18hpi (Fig. 1A). CPE were most prevalent at 24hpi with about 75% of cells remaining viable at the highest MOI (Fig. 1B). By 48hpi only 20% of the cells or less were viable at all MOIs. These results are in agreement with previous studies demonstrating the ability of VEEV to productively infect primary astrocytes (Peng et al., 2013; Schoneboom et al., 1999).

3.2. EGR1 expression is induced following VEEV infection of primary astrocytes

Previously, we demonstrated EGR1 induction following VEEV infection of U87MG astrocytoma cells (Baer et al., 2016). Experiments were performed to determine if EGR1 is also upregulated in VEEV infected primary human astrocytes. Analyses of RT-qPCR data demonstrated that EGR1 was upregulated in VEEV-infected astrocytes compared to mock-infected cells. EGR1 mRNA upregulation was observed starting at 9hpi with a more dramatic upregulation at 18hpi (Fig. 2A). EGR1 gene upregulation also correlated with higher levels of viral RNA production (Fig. 2B). Similarly, EGR1 protein expression was significantly elevated in cells infected at MOI of 5 (mean = 1.526 fold change, p-value equals 0.0002) compared to mock-infected (mean = 1 fold change) or those infected at MOI of 1 (mean = 1.17 fold change) at 18hpi (Fig. 2C and D). These data confirm that EGR1 upregulation is a conserved response to VEEV infection in primary astrocytes.

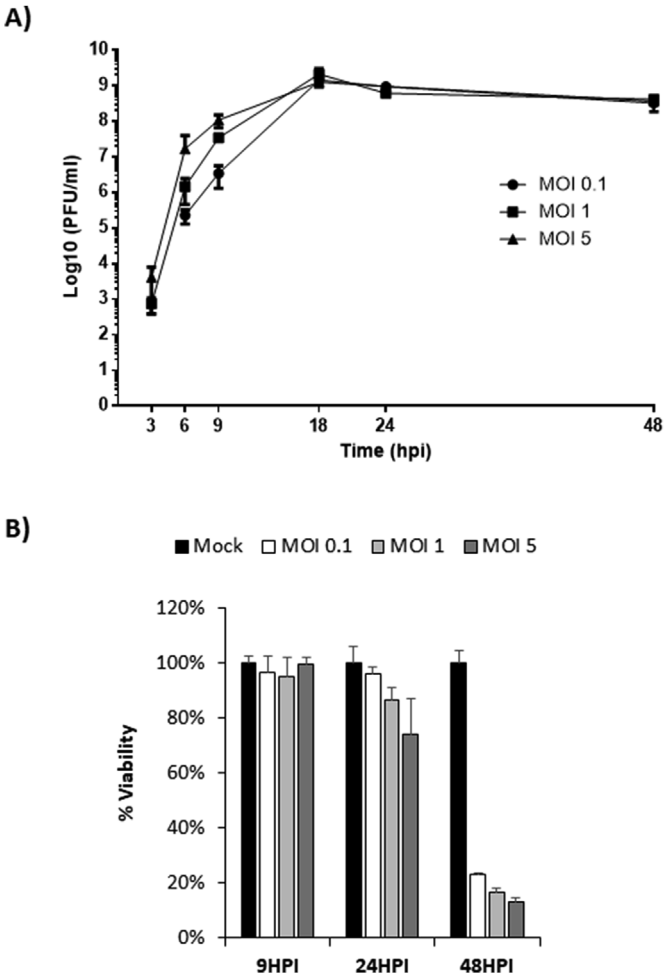

Fig. 1. VEEV replicates efficiently in primary astrocytes. A) Cells were infected with the attenuated strain of VEEV (VEEVTC-83) at multiple MOIs (0.1, 1, and 5). Viral replication was analyzed at 3, 6, 9, 18, 24, and 48hpi via plaque assays. B) Cell viability was determined at 9, 24 and 48hpi using Cell Titer Glo. Mock-infected cells for each timepoint were included as controls and percent viability for mock-infected cells was set to 100%. Data are expressed as the Mean ± SD (n = 3).

3.3. EGR1 expression is dependent on ERK and PERK signaling

VEEV infection of U87MG cells induces the PERK arm of the UPR activating EGR1 mRNA and protein expression leading to VEEV-induced cell death or apoptosis (Baer et al., 2016). However, EGR1 expression can also be stimulated by extracellular signal-regulated kinase (ERK), p38 mitogen activated protein kinase (MAPK) and phosphoinositide 3-kinase (PI3K) pathways (Pagel and Deindl, 2011) and there is significant crosstalk between MAPK signaling and the UPR (Darling and Cook, 2014). To determine if ERK, p38, PI3K, or PERK are necessary for EGR1 induction, we tested well characterized small molecule kinase inhibitors. EGR1 transcripts were significantly downregulated in both mock and VEEV-infected cells treated with an ERK inhibitor (ERKi, PD0325901). Over a 6-fold decrease in EGR1 gene expression (mean = 0.058 fold change) was observed in ERKi treated and VEEV-infected cells compared to DMSO treated and VEEV-infected (mean = 6.35 fold change, p-value equals 0.0001) (Fig. 3A). Similarly, treatment with a

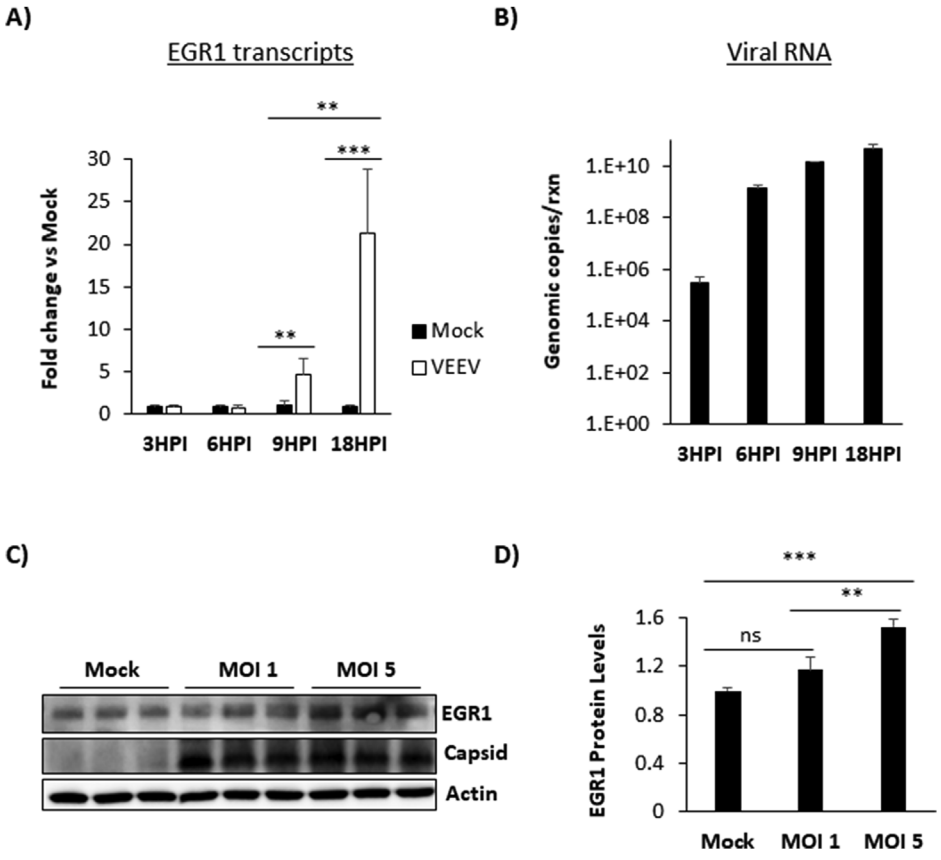

Fig. 2. EGR1 expression is induced following VEEV infection in primary astrocytes. A) Primary astrocytes were infected with VEEV TC-83 at an MOI of 1 and total RNA extracted at 3, 6, 9, and 18hpi. Gene expression was determined using TaqMan assays for EGR1. Fold changes were calculated relative to 18S ribosomal RNA and normalized to mock samples using the ΔΔCt method. B) Cells were infected and RNA extracted as above in panel A. Viral genomic copies were determined by RT-qPCR. Results are displayed as genomic copies in logarithmic scale. C) Astrocytes were mock-infected or infected with TC-83 (MOI 1 or 5) for 1 h. At 18hpi, cell lysates were collected using blue lysis buffer and analyzed by immunoblot. PVDF membranes were probed to determine levels of EGR1 and VEEV capsid. β-Actin was used as a loading control. D) EGR1 protein levels were normalized to β-Actin. Data are expressed as the Mean ± SD (n = 3). *p-value ≤ 0.05, **p-value ≤0.01, ***p-value ≤ 0.001.

PERK inhibitor (PERKi, GSK2606414) also suppressed EGR1 expression in VEEV-infected cells by over four-fold (mean = 3.02 fold change) compared to DMSO treated and VEEV-infected cells (mean = 7.62 fold change, p-value equals 0.0003) (Fig. 3C). Treatment with a p38MAPK inhibitor (p38MAPKi, SB203580) had no significant impact on EGR1 expression (n.s.) (Fig. 3A). Treatment with PI3K inhibitor (PI3Ki, PI-103) elevated EGR1 expression (mean = 17.8 fold change) compared to DMSO treated and VEEV-infected cells (mean = 11.3 fold change, p-value equals 0.049) (Fig. 3B). Overall, these results demonstrate that EGR1 expression is induced following VEEV infection through ERK- and PERK-dependent pathways. Since ERK and PERK inhibitors had a major impact in suppressing EGR1 expression, subsequent studies focused on ERK and PERK pathways.

3.4. Loss of EGR1 reduces VEEV-induced apoptosis and impacts viral replication in primary astrocytes

Since EGR1 is at least partially responsible for VEEV-induced cell death in U87MG astrocytes, the impact of EGR1 on apoptosis in primary astrocytes was assessed. Primary astrocytes were transfected with siRNA targeting EGR1 prior to VEEV infection. At 18hpi, lysates were collected for western blot analysis. EGR1 protein expression was significantly reduced in cells treated with siRNA against EGR1 indicating successful knockdown (Fig. 4A and B). As expected, negative control siRNA (siNeg) transfected and VEEV-infected cells had increased expression of EGR1 compared to siNeg treated and mock-infected cells. A modest, but significant, decrease in viral RNA was observed in siEGR1 transfected and VEEV infected cells by nearly 1 log (mean = 1.7e8 genomic copies) compared to siNeg transfected and VEEV infected cells

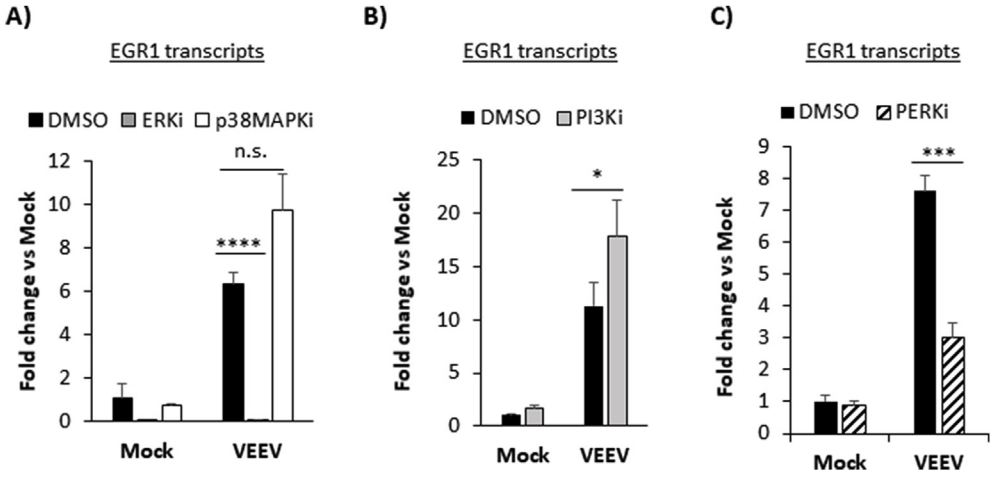

Fig. 3. EGR1 expression is dependent on ERK and PERK signaling. A-C) Primary astrocytes were mock-infected or infected with TC-83 (MOI 5) for 1 h and pre- and post-treated with either DMSO, ERKi (10 μM), p38MAPKi (10 μM), PI3Ki (500 nM), or PERKi (2.5 μM). At 18hpi total RNA was extracted and gene expression was determined using TaqMan assays for EGR1. Fold changes were calculated relative to 18S ribosomal RNA and normalized to mock samples using the ΔΔCt method. Data are expressed as the Mean ± SD (n = 3). *p-value ≤ 0.05, ***p-value ≤ 0.001, ****p-value ≤ 0.0001. n.s. = not significant

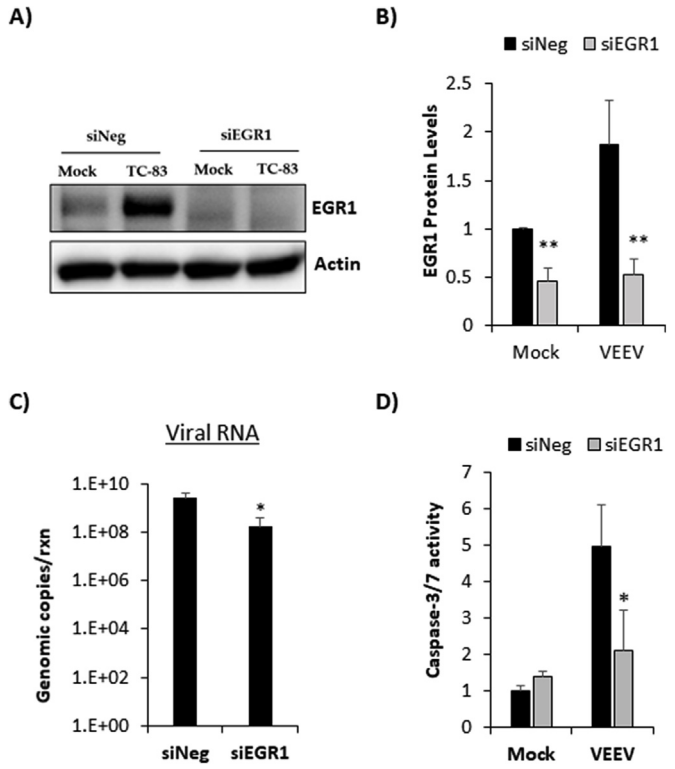

Fig. 4. Loss of EGR1 blocks VEEV-induced apoptosis in primary astrocytes. Primary astrocytes were transfected with a negative-control (siNeg) or siRNA targeting EGR1 (siEGR1) at 50 nM. At 48 h post-transfection, cells were infected with VEEVTC-83 (MOI 5) or mock-infected. At 18hpi, A) Cell lysates were collected using blue lysis buffer and analyzed by western blot. PVDF membranes were probed for levels of EGR1 and β-Actin was used as a loading control. B) EGR1 protein levels were normalized to β-Actin. Data are expressed as the Mean ± SD (n = 3). C) Total RNA was extracted and viral genomic copies were determined by RT-qPCR. Results are displayed as genomic copies in logarithmic scale. Data are expressed as the Mean ± SD (n = 4) D) Caspase-3/7 activity was measured using the Caspase-Glo 3/7 assay (Promega). Data are expressed as the Mean ± SD (n = 4). *p-value ≤ 0.05, **p-value ≤ 0.01.

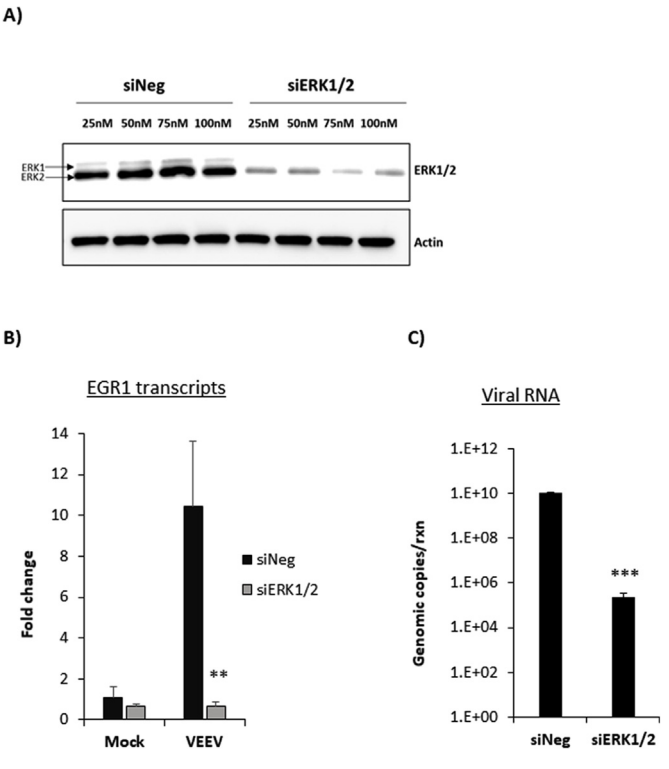

Fig. 5. Knockdown of ERK1/2 decreases EGR1 expression and viral RNA. A) Primary astrocytes were transfected with various concentrations of either negative-control (siNeg) or siRNA targeting ERK1/2 (siERK1/2). At 48 h post transfection, cell lysates were collected in blue lysis buffer and analyzed by western blot. PVDF membranes were probed for levels of ERK1/2 and β-Actin was used as a loading control. B) Cells were transfected with 100 nM siNeg or siERK1/2 siRNAs for 48 h and then infected with VEEV TC-83 (MOI 5) or mock-infected. At 18hpi, total RNA was extracted and gene expression was determined using TaqMan assays for EGR1. Fold changes were calculated relative to 18S ribosomal RNA and normalized to mock samples using the ΔΔCt method. C) RNA collected as described in panel B was used for viral genomic copy determination by RT-qPCR. Results are displayed as genomic copies in logarithmic scale. Data are expressed as the Mean ± SD (n = 3). **p-value ≤0.01, ***p-value ≤ 0.001.

(mean = 2.6e9 genomic copies, p-value equals 0.04) indicating that loss of EGR1 impacts viral replication (Fig. 4C). Increased caspase 3/7 activity was observed following VEEV infection and loss of EGR1 in VEEV infected cells significantly reduced caspase 3/7 activity by more than 2-fold compared to cells transfected with siNeg (Fig. 4D). These data indicate that loss of EGR1 limits viral induced apoptosis in primary astrocytes in addition to impacting viral replication.

3.5. ERK1/2 siRNA reduces EGR1 expression and significantly impacts viral replication

To confirm that EGR1 expression was dependent on the ERK pathway and to determine its impact on viral replication, siRNA knockdown against ERK1/2 was performed. At 48 h post transfection, lysates were collected for western blot analysis. ERK1/2 protein expression was significantly reduced in cells treated with each concentration of ERK1/2 siRNA tested, indicating a successful knockdown of ERK1/2 (Fig. 5A). To ensure a robust knockdown, 100 nM of siRNA was selected for subsequent studies. siRNA transfection was followed by mock or VEEV infection and at 18hpi total RNA was extracted to determine EGR1 expression. siERK1/2 transfected and VEEV infected cells had a significant and dramatic decrease in EGR1 mRNA expression by nearly 10-fold (mean = 0.65 fold change) compared to siNeg and TC-83 infected cells (mean = 10.4 fold change) (p-value equals 0.006) (Fig. 5B) indicating that EGR1 expression is dependent on the ERK pathway. Similarly, a significant and dramatic decrease (about 5 log) in viral RNA was observed in siERK1/2 transfected cells (mean = 2.2e5 genomic copies) compared to siNeg transfected cells (mean = 1.02e10 genomic copies, p-value equals 0.0001) (Fig. 5C). These data confirm that ERK is important for induction of EGR1 gene expression and that downregulating ERK1/2 reduces VEEV viral RNA production.

3.6. PERK siRNA reduces EGR1 expression and significantly impacts viral replication

We further tested if knockdown of PERK would have a similar impact on EGR1 as well as viral replication. Cells were transfected with siNeg or PERK siRNA at increasing concentrations. Lysates were collected at 48 h post transfection and PERK expression was analyzed by western blot analysis. PERK protein expression was significantly reduced in cells transfected with each concentration of siPERK tested, indicating successful knockdown of PERK (Fig. 6A). To ensure a robust knockdown, 100 nM of siRNA was selected for subsequent studies. We next assessed the levels of EGR1 mRNA expression in cells transfected with siPERK and infected with VEEV. Similar to the siERK1/2 data, knockdown of PERK significantly reduced EGR1 expression by nearly 10-fold in VEEV-infected cells (mean = 0.74 fold change) compared to siNeg transfected and VEEV infected cells (mean = 10.26 fold change, p-value equals 0.0001). Likewise, viral RNA decreased by nearly 5 log

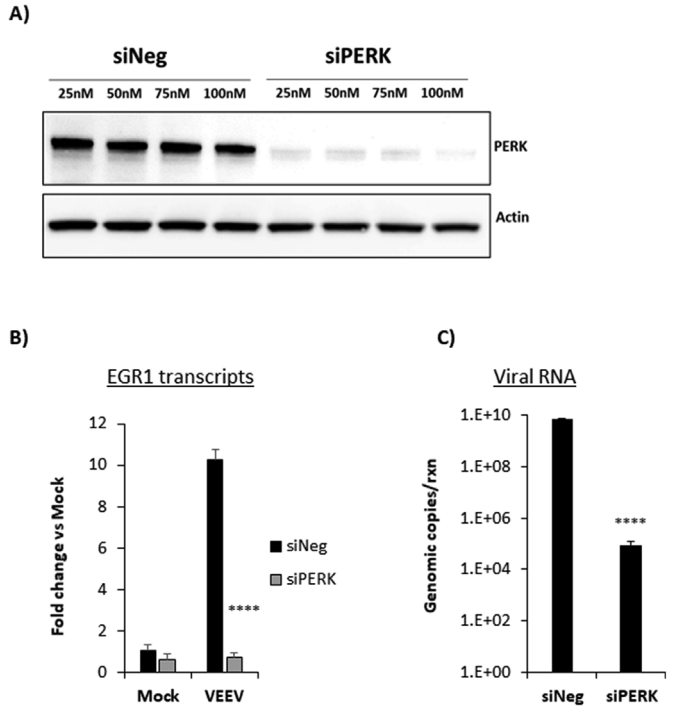

Fig. 6. Knockdown of PERK decreases EGR1 expression and viral RNA. A) Primary astrocytes were transfected with various concentrations of a negative-control (siNeg) or siRNA targeting PERK (siPERK). At 48 h post transfection, cell lysates were collected using blue lysis buffer and analyzed by western blot. PVDF membranes were probed for levels of ERK1/2 and β-Actin as a loading control. B) Cells were transfected with 100 nM siNeg or siPERK siRNAs for 48 h and then infected with VEEV-TC83 (MOI 5) or mock-infected. At 18hpi, total RNA was extracted and gene expression was determined using TaqMan assays for EGR1 gene. Fold changes were calculated relative to 18S ribosomal RNA and normalized to mock samples using the ΔΔCt method. C) RNA collected as described in panel B was used for viral genomic copy determination by RT-qPCR. Results are displayed as genomic copies in logarithmic scale. Data are expressed as the Mean ± SD (n = 3). **p-value ≤0.01, ****p-value ≤ 0.0001.

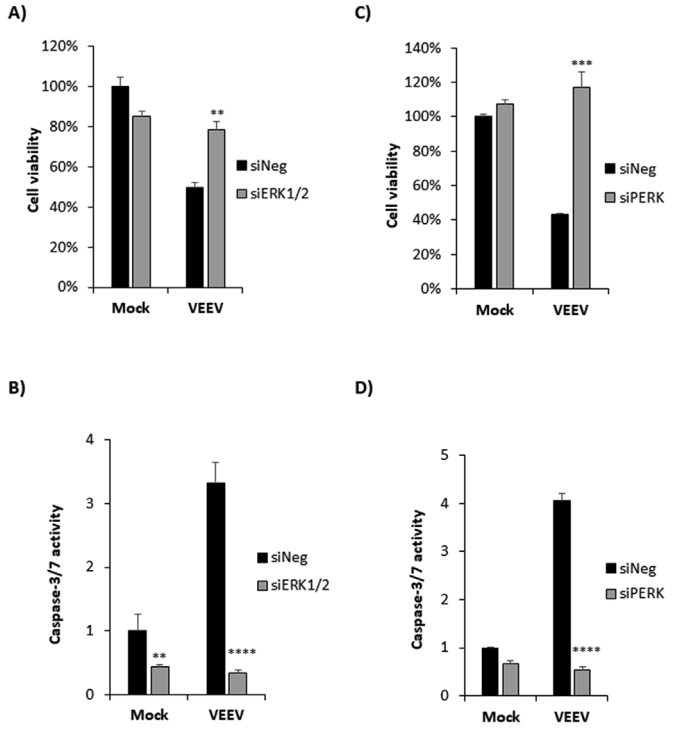

Fig. 7. Knockdown of ERK1/2 or PERK increases cell viability as well as rescues cells from VEEV induced apoptosis. Primary astrocytes were transfected with siNeg, siERK1/2, or siPERK siRNAs at 100 nM. At 48 h post transfection, cells were infected with VEEV-TC83 (MOI 5) or mock-infected and at 36hpi, A and C) Percent cell viability was measured using CellTiter-Glo assay. B and D) Caspase-3/7 activity was measured using Caspase-Glo 3/7 assay. Data was normalized to siNeg-transfected and mock-infected cells. Data are expressed as the Mean ± SD (n = 3). **p-value ≤0.01, ***p-value ≤ 0.001, ****p-value ≤ 0.0001.

fold in siPERK transfected and VEEV infected cells (mean = 8.7e4 genomic copies) compared to siNeg-transfected and VEEV-infected cells (mean = 6.8e9 genomic copies) (p-value equals 0.0001). These data indicate that EGR1 expression is also regulated by PERK and loss of PERK decreases VEEV viral RNA production.

3.7. Loss of ERK1/2 or PERK increases cell viability and blocks VEEV induced apoptosis in VEEV infected astrocytes

Since blocking either the ERK or the PERK pathway had a major impact on EGR1 expression as well as VEEV replication in primary astrocytes, we next assessed the impact of loss of ERK1/2 and PERK on cell survival following VEEV infection. Cells were transfected with siRNAs targeting ERK1/2, PERK, or siNeg followed by VEEV infection. At 36hpi, cell viability was measured using the CellTiter Glo assay and caspase 3/7 activity was measured using the Caspase-Glo 3/7 assay. Less than 50% of cells were viable in siNeg-transfected and VEEV-infected cells (Fig. 7A and C). Cells transfected with siERK1/2 and VEEV-infected had cell viability over 78% (p value equals 0.003) (Fig. 7A). Similarly, cells transfected with siPERK and VEEV-infected had a significant improvement in cell viability (Fig. 7C). Caspase-3/7 activity was highly impacted in cells transfected with siERK1/2 or siPERK and VEEV-infected. A dramatic reduction in VEEV induced apoptosis was observed in siERK1/2 transfected cells by nearly 3-fold compared to siNeg-transfected cells (p-value equals 0.0001) (Fig. 7B). Similarly, nearly 4-fold reduction in VEEV induced apoptosis was observed in siPERK transfected and VEEV-infected cells compared to siNeg transfected and VEEV-infected cells (p-value equals 0.0001). No visible CPE was evident in siERK1/2 or siPERK transfected and VEEV infected cells even after 36hpi when observed under microscope (data not shown). These data indicate that loss of PERK and ERK impedes VEEV induced cell death.

4. Discussion

Astrocytes and neurons are the primary targets of VEEV in the brain (Cain et al., 2017) inducing well-characterized cytopathic effects in neurons of the CNS. In this study, we showed that VEEV replication in human primary astrocytes and the apoptosis induced following VEEV infection can be suppressed by blocking either ERK or PERK pathways, both of which are responsible for upregulating EGR1 pathway, rescuing the cells from VEEV induced apoptosis. Cytopathic effects in primary astrocytes following VEEV infection has been shown in previous published studies (Peng et al., 2013; Schoneboom et al., 1999). Substantial amounts of astrocyte cell death due to VEEV-astrocyte interaction could contribute to decreased neuronal survival and long-term CNS damage.

We demonstrated that EGR1 expression is increased following VEEV TC83 infection in human primary astrocytes at both the mRNA and protein levels. These studies are in agreement with our previous study which showed that EGR1 upregulation contributed to VEEV TrD-induced apoptosis in U87MG astrocytoma cells (Baer et al., 2016). A caveat of our current work is that all of our data were produced using infection of primary astrocytes with VEEV TC-83. VEEV TC-83 is a live attenuated vaccine strain of VEEV that has investigational new drug status and can only be used for vaccination of animals and individuals, such as military personnel, that are at risk for VEEV exposure (Sharma and Knollmann-Ritschel, 2019). While VEEV TC-83 replicates

efficiently *in vitro,* it has limited pathogenicity in mouse models of infection with most strains of mice surviving infection and displaying less severe brain pathology as compared to VEEV TrD infection (Steele et al., 1998; Hyde et al., 2014). However, our current data coupled with our previous work indicate that EGR1 upregulation and its subsequent induction of apoptosis are induced by both VEEV TC-83 and TrD infections.

Our data also indicate that EGR1 expression following VEEV infection was dependent on both the ERK and PERK signaling pathways which was determined by inhibitor treatments and confirmed by siRNA transfections. ERK signaling is a central MAPK pathway and ERK proteins are critical members of the Ras-Raf-MEK-ERK signaling pathway, activated by various stimuli, and play an important role in cell proliferation, differentiation, survival, learning, and sometimes apoptosis (Shaul and Seger, 2007). The ERK proteins are abundantly expressed throughout the brain (Zsarnovszky and Belcher, 2004) and the ERK pathway has been shown to activate EGR1 induced by nerve-growth factor, which in turn mediates p35 induction, leading to neuronal differentiation (Harada et al., 2001). Activated ERK is known to phosphorylate serine/threonine residues of more than 50 downstream cytosolic and nuclear substrates (Seger and Krebs, 1995; Pearson et al., 2001). Amoung these substrates, ERK phosphorylates the transcription factor Elk-1 (Cargnello and Roux, 2011), which in turn induces EGR1 gene expression (Tur et al., 2010; Duclot and Kabbaj, 2017b). Previous work has shown the MAPK transduction pathways as key players in the cell death of rat cortical astrocytes (Fernandes et al., 2007), which is in agreement with our results. EGR1 activation and upregulation via the ERK signaling cascade has also been observed in melanoma cells (Gaggioli et al., 2005), prostate cancer cells (Gregg and Fraizer, 2011), and in breast cancer cell lines (Wenzel et al., 2007), implying that EGR1 induction may be a conserved stress response not only in astrocytes, but also other cell types.

The UPR maintains the homeostasis of cellular proteins by preventing the excessive accumulation of misfolded or unfolded proteins in the lumen of the ER during normal and aberrant conditions (Rathore et al., 2013). The PERK pathway of the UPR, is involved in both survival and apoptotic signaling. PERK-mediated phosphorylation of eIF2α prevents ER stress-induced apoptosis whereas, under severe cell ER stress, the PERK-eIF2α-ATF4 pathway activates transcription of pro-apoptotic factors, such as C/EBP homologous protein (CHOP) and growth arrest and DNA damage-inducible protein GADD34 enhancing apoptosis signaling (Kadowaki and Nishitoh, 2013; Novoa et al., 2003). Indeed, in VEEV-infected U87MG cells, CHOP expression was induced (Baer et al., 2016). Our data suggest that PERK activity is stimulated following infection due to the accumulation of large amounts of viral glycoproteins in the ER causing ER stress which can activate UPR signaling cascades (Steele et al., 1998), ultimately leading to EGR1 activation in infected cells (Bender et al., 2012).

Our results showed that even though suppressing EGR1 had an impact on viral replication as well as rescued astrocytes from VEEV induced cell death, blocking the ERK or the PERK pathway had a more dramatic effect on viral replication. Inhibition of ERK signaling through small molecule inhibitors was previously shown to suppress VEEV replication (Voss et al., 2014), supporting the importance of the ERK pathway for VEEV replication. These data indicate that blocking EGR1 alone is not sufficient to dramatically impact VEEV replication, in agreement with our previous data where VEEV TrD replication in wildtype and EGR1 −/− mouse embryonic fibroblasts (MEFs_) was comparable (Baer et al., 2016). Given that ERK phosphorylates more than 50 substrates (Seger and Krebs, 1995; Pearson et al., 2001) and PERK stimulates multiple signaling components including other transcription factors (ATF4, Nrf2, CHOP (Hughes and Mallucci, 2019)) the observed impact on viral replication may be peripheral to their regulation of EGR1 gene expression. Alternatively, since a modest impact on viral replication was observed following loss of EGR1, a combination of multiple ERK or PERK regulated factors may be needed to strongly impact VEEV replication. However, loss of EGR1 was sufficient to reduce VEEV induced apoptosis, indicating that its role is related to regulation of cell death pathways rather than impacting viral replication.

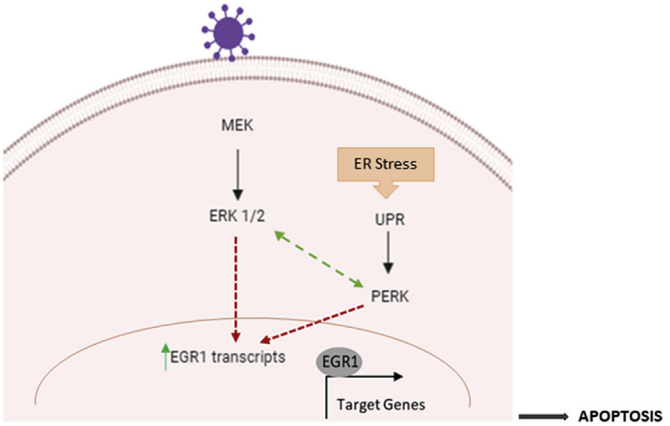

Fig. 8. Proposed model of EGR1 regulated human primary astrocyte cell death following VEEV infection. Following VEEV infection of astrocytes, the ERK signaling cascade is activated. The PERK arm of the UPR is also induced due to the accumulation of viral glycoproteins with the ER. Both ERK and PERK pathways contribute to the induction of EGR1 (at the transcription level). EGR1 contributes to VEEV induced cell death through an undetermined mechanism, which is likely due to transcriptional regulation of apoptotic factors.

Taken together, our data leads to a proposed model of EGR1 regulated astrocyte cell death following VEEV infection (Fig. 8). On one hand, VEEV infection leads to activation of the ERK signaling cascade in cells (Voss et al., 2014), activating EGR1 gene expression. While on the other hand, viral infection leads to ER stress in cells, activating the PERK arm of the UPR pathway which in turn contributes to EGR1 activation. (Baer et al., 2016). Previous studies have shown significant cross talk between ERK signaling and endoplasmic reticulum stress in cancer, atherosclerosis, and ischemia. During ER stress, PERK and ATF6 promote ERK and p38 phosphorylation thus boosting pro-inflammatory cytokine secretion in bronchial epithelial cells (Mijošek et al., 2016). However, ERK phosphorylation is induced at early time points (5 min to 6 h) following VEEV infection, suggesting that there is an early induction of ERK activity (Voss et al., 2014) and a later ER stress stimulated ERK activity in VEEV infected cells. Activated EGR1 then translocates to the nucleus leading to the activation of various EGR1 regulated genes ultimately contributing to apoptosis. Blocking the ERK or PERK pathways suppresses EGR1 gene expression, which in turn can block viral-induced apoptosis leading to cell survival. The mechanism by which EGR1 contributes to apoptosis is largely unknown. Ongoing studies in our lab are aimed at identifying EGR1 responsive genes to begin to elucidate EGR1-dependent gene expression changes that contribute to VEEV-induced cell death.

Declaration of competing interest

Author Jonathan Jacobs is employed by the company Qiagen. The remaining authors declare that the research was conducted in the absence of any commercial or financial relationships that could be construed as a potential conflict of interest.

Acknowledgements

Fig. 8 was created with BioRender. This work was funded through Defense Threat Reduction Agency (DTRA) grant HDTRA1-18-1-0045 to KKH, US Department of the Navy N00173-17-1-G006 to MVH/KKH and HDTRA1-5-1-7467 to AAA. Funders do not have any role in the design of the study and collection, analysis, and interpretation of data and nor

in writing the manuscript.

References

Aronson, J.F., et al., 2000. A single-site mutant and revertants arising in vivo define early steps in the pathogenesis of Venezuelan equine encephalitis virus. Virology 270 (1), 111–123.

Au - Baer, A., Au - Kehn-Hall, K., 2014. Viral concentration determination through plaque assays: using traditional and novel overlay systems. J. Vis. Exp.(93), e52065.

Austin, D., et al., 2012. p53 activation following rift valley fever virus infection contributes to cell death and viral production. PLoS One 7 (5), e36327.

Baer, A., et al., 2016. Venezuelan equine encephalitis virus induces apoptosis through the unfolded protein response activation of EGR1. J. Virol. 90 (7), 3558–3572.

Bender, C., et al., 2012. Role of Astrocytes in Viral Infections. pp. 1–2.

Cain, M.D., et al., 2017. Virus entry and replication in the brain precedes blood-brain barrier disruption during intranasal alphavirus infection. J. Neuroimmunol. 308, 118–130.

Cargnello, M., Roux, P.P., 2011. Activation and function of the MAPKs and their substrates, the MAPK-activated protein kinases. Microbiol. Mol. Biol. Rev. 75 (1), 50–83.

Croddy, E., Chemical and Biological Warfare: a Comprehensive Survey for the Concerned Citizen. xxii, 306 pages.

Darling, N.J., Cook, S.J., 2014. The role of MAPK signalling pathways in the response to endoplasmic reticulum stress. Biochim. Biophys. Acta 1843 (10), 2150–2163.

Duclot, F., Kabbaj, M., 2017a. The role of early growth response 1 (EGR1) in brain plasticity and neuropsychiatric disorders. Front. Behav. Neurosci. 11 35-35.

Duclot, F., Kabbaj, M., 2017b. The role of early growth response 1 (EGR1) in brain plasticity and neuropsychiatric disorders. Front. Behav. Neurosci. 11.

Fan, Y., et al., 2011. Activation of Egr-1 expression in astrocytes by HIV-1 Tat: new insights into astrocyte-mediated Tat neurotoxicity. J Neuroimmune Pharmacol 6 (1), 121–129 PMID: 20414733.

Fernandes, A., et al., 2007. MAPKs are key players in mediating cytokine release and cell death induced by unconjugated bilirubin in cultured rat cortical astrocytes. Eur. J. Neurosci. 25 (4), 1058–1068.

Franz, D.R., et al., 2001. Clinical recognition and management of patients exposed to biological warfare agents. Clin. Lab. Med. 21 (3), 435–473.

Gaggioli, C., et al., 2005. HGF induces fibronectin matrix synthesis in melanoma cells through MAP kinase-dependent signaling pathway and induction of Egr-1. Oncogene 24 (8), 1423–1433.

Gregg, J., Fraizer, G., 2011. Transcriptional regulation of EGR1 by EGF and the ERK signaling pathway in prostate cancer cells. Genes Cancer 2 (9), 900–909.

Grieder, F.B., et al., 1995. Specific restrictions in the progression of Venezuelan equine encephalitis virus-induced disease resulting from single amino acid changes in the glycoproteins. Virology 206 (2), 994–1006.

Hanson, R.P., et al., 1967. Arbovirus infections of laboratory workers. Extent of problem emphasizes the need for more effective measures to reduce hazards. Science 158 (3806), 1283–1286.

Harada, T., et al., 2001. ERK induces p35, a neuron-specific activator of Cdk5, through induction of Egr1. Nat. Cell Biol. 3, 453.

Hughes, D., Mallucci, G.R., 2019. The unfolded protein response in neurodegenerative disorders - therapeutic modulation of the PERK pathway. FEBS J. 286 (2), 342–355.

Hyde, J.L., et al., 2014. A viral RNA structural element alters host recognition of nonself RNA. Science 343 (6172), 783–787.

Kadowaki, H., Nishitoh, H., 2013. Signaling pathways from the endoplasmic reticulum and their roles in disease. Genes 4 (3), 306–333.

Kim, D.Y., et al., 2011. Conservation of a packaging signal and the viral genome RNA packaging mechanism in alphavirus evolution. J. Virol. 85 (16), 8022–8036.

Kinney, R.M., et al., 1993. Attenuation of Venezuelan equine encephalitis virus strain TC-83 is encoded by the 5'-noncoding region and the E2 envelope glycoprotein. J. Virol. 67 (3), 1269–1277.

Mijošek, V., et al., 2016. Endoplasmic reticulum stress is a danger signal promoting innate inflammatory responses in bronchial epithelial cells. J. Innate Immun. 8 (5), 464–478.

Novoa, I., et al., 2003. Stress-induced gene expression requires programmed recovery from translational repression. EMBO J. 22 (5), 1180–1187.

Paessler, S., Weaver, S.C., 2009. Vaccines for Venezuelan equine encephalitis. Vaccine 27 (Suppl. 4), D80–D85.

Pagel, J.I., Deindl, E., 2011. Early growth response 1–a transcription factor in the crossfire of signal transduction cascades. Indian J. Biochem. Biophys. 48 (4), 226–235.

Pearson, G., et al., 2001. Mitogen-activated protein (MAP) kinase pathways: regulation and physiological functions*. Endocr. Rev. 22 (2), 153–183.

Peng, B.-H., et al., 2013. Production of IL-8, IL-17, IFN-gamma and IP-10 in human astrocytes correlates with alphavirus attenuation. Vet. Microbiol. 163 (3), 223–234.

Rathore, A.P.S., Ng, M.-L., Vasudevan, S.G., 2013. Differential unfolded protein response during Chikungunya and Sindbis virus infection: CHIKV nsP4 suppresses eIF2α phosphorylation. Virol. J. 10 (1), 36.

Schäfer, A., et al., 2011. The role of the blood-brain barrier during Venezuelan equine encephalitis virus infection. J. Virol. 85 (20), 10682–10690.

Schoneboom, B.A., et al., 1999. Astrocytes as targets for Venezuelan equine encephalitis virus infection. J. Neurovirol. 5 (4), 342–354.

Schoneboom, B.A., Lee, J.S., Grieder, F.B., 2000. Early expression of IFN-alpha/beta and iNOS in the brains of Venezuelan equine encephalitis virus-infected mice. J. Interferon Cytokine Res. 20 (2), 205–215.

Seger, R., Krebs, E.G., 1995. The MAPK signaling cascade. FASEB J. 9 (9), 726–735.

Sharma, A., Knollmann-Ritschel, B., 2019. Current understanding of the molecular basis of Venezuelan equine encephalitis virus pathogenesis and vaccine development. Viruses 11 (2).

Shaul, Y.D., Seger, R., 2007. The MEK/ERK cascade: from signaling specificity to diverse functions. Biochim. Biophys. Acta Mol. Cell Res. 1773 (8), 1213–1226.

Steele, K.E., et al., 1998. Comparative neurovirulence and tissue tropism of wild-type and attenuated strains of Venezuelan equine encephalitis virus administered by aerosol in C3H/HeN and BALB/c mice. Vet. Pathol. 35 (5), 386–397.

Tur, G., et al., 2010. Factor binding and chromatin modification in the promoter of murine Egr1 gene upon induction. Cell. Mol. Life Sci. 67 (23), 4065–4077.

Voss, K., et al., 2014. Inhibition of host extracellular signal-regulated kinase (ERK) activation decreases new world alphavirus multiplication in infected cells. Virology 468–470, 490–503.

Weaver, Scott C., et al., 2004. Venezuelan equine encephalitis. Annu. Rev. Entomol. 49 (1), 141–174.

Wenzel, K., et al., 2007. Expression of the protein phosphatase 1 inhibitor KEPI is downregulated in breast cancer cell lines and tissues and involved in the regulation of the tumor suppressor EGR1 via the MEK-ERK pathway. Biol. Chem. 388 (5), 489–495.

Zsarnovszky, A., Belcher, S.M., 2004. Spatial, temporal, and cellular distribution of the activated extracellular signal regulated kinases 1 and 2 in the developing and mature rat cerebellum. Dev. Brain Res. 150 (2), 199–209.